

JOSEPHSON JUNCTION QUBITS WITH SYMMETRIZED COUPLINGS TO A RESONANT LC BUS

Stanford P. Yukon

1. INTRODUCTION

The system for quantum computation(QC) that we are proposing is modeled on the ion trap system for QC¹ where the ion qubits are coupled among themselves through their collective oscillations in the ion trap, which plays the role of a resonant bus. The bus for the proposed Josephson junction(JJ) prism qubit QC is a single mode LC resonant loop^{2,3,4}. Magnetic flux from the loop threading a qubit will produce a loop-qubit interaction via the Bohm Aharonov effect. At their preferred operating point, the proposed qubits have negligible circulating persistent currents and are kept by symmetry from interacting with their coupled measurement SQUIDS. By pairing the physical qubits into logical qubits, it is possible to maintain the logical qubits in a decoherence free subspace(DFS)^{5,6,7} that nulls the decoherence effects of uniform external flux perturbations, and the perturbations associated with computational Mølmer Sørensen(MS) bichromatic gates^{8,9,10}. The only time a logical qubit should interact with the environment is during the unitary gate rotation that initialize the qubits, and during the final Hadamard rotation, which allows the qubit to interact with the measurement SQUID gradiometer.

2. JOSEPHSON JUNCTION TRIANGULAR PRISM QUBITS

The physical qubits that we shall consider are based on a simplified version of qubits considered in a previous paper⁴. We assume that the junction critical currents and the circuit dimensions are small enough so that the dimensionless self and mutual inductances of the qubit circuit in units of $L_c = \Phi_0 / (2\pi I_c)$ are small and can be neglected^{11,12}. The Hamiltonian for the qubit shown in Fig. 1 may be written in term of the junction gauge invariant phases ζ_i , critical currents J_{C_i} , and capacitances C_i as

$$H = \sum_{i=1}^4 \left[\frac{1}{2} \zeta_i^2 (\Phi_0 / 2\pi)^2 / C_i - E_J (J_{C_i} / J_c) \cos(\zeta_i) \right]$$
 where the flux quantum and junction characteristic energy are written as $\Phi_0 = h / 2e$ and $E_J = J_c \Phi_0 / 2\pi$.

The phase constraint equations for the two cells are given by $\zeta_1 - \zeta_2 - \zeta_3 = \phi_{a1}$ and $\zeta_2 - \zeta_1 + \zeta_4 = \phi_{a2}$. Defining the symmetric and antisymmetric combinations of the external magnetic fluxes and phases as $\theta = (\zeta_1 + \zeta_2) / 2$, $\psi = (\zeta_1 - \zeta_2) / 2$ and $\phi_s = \frac{1}{2}(\phi_{a1} + \phi_{a2})$, $\phi_a = \frac{1}{2}(\phi_{a1} - \phi_{a2})$, with $\phi_i = 2\pi(\Phi_i / \Phi_0)$ yields $\zeta_3 = 2\psi - \phi_a - \phi_s$ and $\zeta_4 = 2\psi - \phi_a + \phi_s$. We allow for the possibility of differing junction areas by writing $J_{C_{1,2}} = J \pm \Delta J$, $J_{C_{3,4}} = j \pm \Delta j$, $C_{1,2} = C \pm \Delta C$, and $C_{3,4} = \bar{C} \pm \Delta \bar{C}$.

In order to obtain the unperturbed Hamiltonian and its wave function, we assume

REPORT DOCUMENTATION PAGE

*Form Approved
OMB No. 0704-0188*

The public reporting burden for this collection of information is estimated to average 1 hour per response, including the time for reviewing instructions, searching existing data sources, gathering and maintaining the data needed, and completing and reviewing the collection of information. Send comments regarding this burden estimate or any other aspect of this collection of information, including suggestions for reducing the burden, to Department of Defense, Washington Headquarters Services, Directorate for Information Operations and Reports (0704-0188), 1215 Jefferson Davis Highway, Suite 1204, Arlington, VA 22202-4302. Respondents should be aware that notwithstanding any other provision of law, no person shall be subject to any penalty for failing to comply with a collection of information if it does not display a currently valid OMB control number.

PLEASE DO NOT RETURN YOUR FORM TO THE ABOVE ADDRESS.

1. REPORT DATE (DD-MM-YYYY) 01-05-2005		2. REPORT TYPE Journal Article		3. DATES COVERED (From - To) 2003	
4. TITLE AND SUBTITLE Josephson junction qubits with symmetrized couplings to a resonant LC bus				5a. CONTRACT NUMBER N/A	
				5b. GRANT NUMBER N/A	
				5c. PROGRAM ELEMENT NUMBER 61102F	
6. AUTHOR(S) Stanford P. Yukon				5d. PROJECT NUMBER 2304	
				5e. TASK NUMBER HE	
				5f. WORK UNIT NUMBER 2304HE03	
7. PERFORMING ORGANIZATION NAME(S) AND ADDRESS(ES) Electromagnetic Scattering Branch (AFRL/SNHE) Source Code: 437890 Electromagnetic Technology Division, Sensors Directorate 80 Scott Drive, Hanscom AFB, MA 01731-2909				8. PERFORMING ORGANIZATION REPORT NUMBER N/A	
9. SPONSORING/MONITORING AGENCY NAME(S) AND ADDRESS(ES) Air Force Office of Scientific Research/NM 875 North Randolph Street Arlington, VA 22203				10. SPONSOR/MONITOR'S ACRONYM(S) AFOSR/NM	
				11. SPONSOR/MONITOR'S REPORT NUMBER(S) AFRL-SN-HS-JA-2004-0490	
12. DISTRIBUTION/AVAILABILITY STATEMENT UNLIMITED DISTRIBUTION					
13. SUPPLEMENTARY NOTES ESC Public Affairs Clearance #: 04-0490; Published in "Quantum Computing and Quantum Bits in Mesoscopic Systems", A. J. Leggett, B. Ruggiero, and P. Silvestrini eds. Kluwer Academic Plenum Publishers, NY USA, (2003)					
14. ABSTRACT The system for quantum computation(QC) we are proposing is modeled on the ion trap system for QC1 where ion qubits are coupled among themselves through collective oscillations in the ion trap, which plays the role of a resonant bus. The bus for the proposed Josephson junction(JJ) prism qubit QC is a single mode LC resonant loop. Magnetic flux from the loop threading a qubit will produce a loop-qubit interaction via the Bohm Aharonov effect. At their preferred operating point, the proposed qubits have negligible circulating persistent currents and are kept by symmetry from interacting with their coupled measurement SQUIDS. By pairing the physical qubits into logical qubits, it is possible to maintain the logical qubits in a decoherence free subspace(DFS) that nulls decoherence effects of uniform external flux perturbations, and perturbations associated with computational Mølmer Sørensen (MS) bichromatic gates. The only time a logical qubit should interact with the environment is during unitary gate rotation that initialize qubits, and during final Hadamard rotation, which allows the qubit to interact with the measurement SQUID gradiometer.					
15. SUBJECT TERMS Josephson junction qubit, geometric gates, holonomic quantum computation.					
16. SECURITY CLASSIFICATION OF:			17. LIMITATION OF ABSTRACT UU	18. NUMBER OF PAGES 12	19a. NAME OF RESPONSIBLE PERSON Stanford. P Yukon
a. REPORT U	b. ABSTRACT U	c. THIS PAGE U			19b. TELEPHONE NUMBER (Include area code)

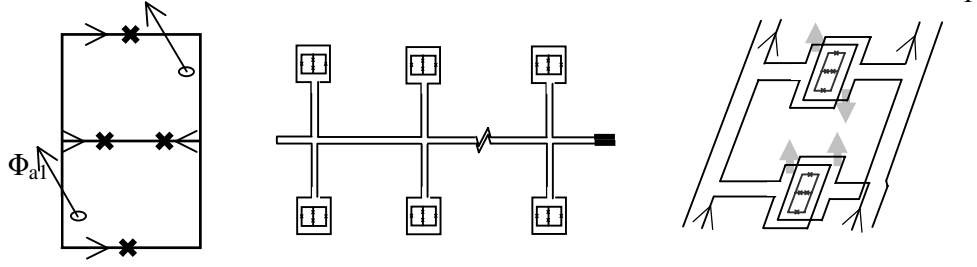


Figure 1. a) JJ prism qubit with junction critical currents J_C , gauge invariant phases ζ_i and external magnetic fluxes Φ_i indicated. b) Resonant LC bus symmetrically coupled to qubit pairs. c) Antisymmetric coupling of adjacent buses to a logical transfer qubit.

equal area junctions and circuit loops, zero external antisymmetric flux, and a constant symmetric flux given by $\Phi_s^0 = (\phi_s^0 / 2\pi)\Phi_0$. The Hamiltonian may be written using θ and ψ variables as

$$H_0(\theta, \psi) = \frac{1}{2}M_\theta \dot{\theta}^2 + \frac{1}{2}M_\psi \dot{\psi}^2 - E_J [2\cos(\theta)\cos(\psi) + 2(j/J)\cos(\phi_s^0)\cos(2\psi - \phi_a)] \quad (1)$$

where we have defined $M_\psi = 2C(1+4\rho)(\Phi_0/2\pi)^2 = (1+4\rho)\hbar^2/4E_c$, $\rho = \bar{C}/C$, $M_\theta = 2C(\Phi_0/2\pi)^2 = \hbar^2/4E_c$, with the capacitive energy E_c given by $E_c = e^2/2C$. A contour plot of the potential energy $V(\theta, \psi) = -2\cos(\theta)\cos(\psi) + r\cos(2\psi - \phi_a)$ is shown in Fig. (2a) for $r = 0.675$ where $r = -2(j/J)\cos(\phi_s^0)$. Approximate eigensolutions are obtained by making a Hartree approximation, where the full two dimensional wave function is approximated by a separable wave function $\Psi(\theta, \psi) \approx \Theta(\theta)\Psi(\psi)$. Assuming that the motion in the θ direction is in its ground state, the $\cos(\theta)$ term in $V(\theta, \psi)$ may be replaced by its expectation value $\eta_H = \langle 0_\theta | \cos(\theta) | 0_\theta \rangle$, leading to an effective qubit potential in ψ given by $V_0(\psi) = -2\eta_H \cos(\psi) + r\cos(2\psi)$. Writing $\dot{\theta}$ and $\dot{\psi}$ in terms of the momentum operators $M_\theta \dot{\theta} = p_\theta = -i\hbar\partial/\partial\theta$, $M_\psi \dot{\psi} = p_\psi = -i\hbar\partial/\partial\psi$ with $m_\psi = M_\psi E_J / \hbar^2$, the unperturbed effective 1D Hamiltonian leads to the time independent Schrödinger equation

$$-\partial^2\Psi(\psi)/\partial\psi^2 - 2m_\psi [2\eta_H \cos(\psi) - r\cos(2\psi)]\Psi(\psi) = 2m_\psi(E_i/E_J)\Psi(\psi) \quad (2)$$

which is in the form of the Whittaker Hill equation. Solutions for the eigen functions and energies for the Whittaker Hill equation have been found by Unwin and Arscott terms of continued fractions¹³.

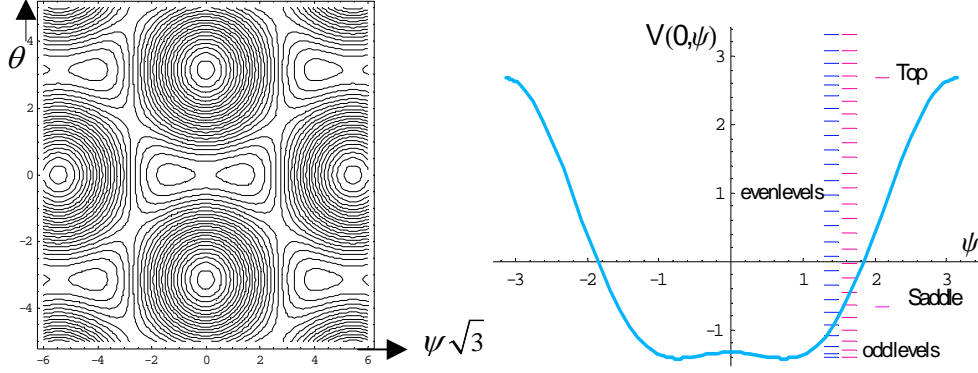


Figure 2. a) Contour plot of $V(\theta, \psi)$ for $r = .675$ b) Energy levels for $V(0, \psi)$ in units of E_J .

3. COUPLING THE RESONANT LC BUS TO THE QUBITS

The qubits are coupled among themselves via their (symmetric) mutual inductance coupling with a resonant LC bus as shown in Fig. (1b). The Hamiltonian for a bus oscillator with inductance L and capacitance C may be written in terms of the phase operators ϕ_s and p_s as $H^{osc}/(\Phi_0/2\pi)^2 = p_s^2/2M_\phi + M_\phi\omega_{LC}^2\phi_s^2/2$ with $M_\phi = C(\Phi_0/2\pi)^2$, $\omega_{LC} = 1/\sqrt{LC}$, and $M_\phi\dot{\phi}_s = p_s = -i\partial/\partial\phi_s$. In terms of annihilation and creation operators $\phi_s = \sqrt{\hbar/2M_\phi\omega_{LC}}(a + a^\dagger)$ and $p_s = i\sqrt{M_\phi\hbar\omega_{LC}/2}(a^\dagger - a)$. In order to carry out unitary qubit gates on the i^{th} qubit, we include an external microwave pulse $\delta\phi_a^{(i)}(t)$ to be added to $\phi_a^{(i)0}$, as well as an external microwave or DC pulse $\delta\phi_{s,ext}^{(i)}(t)$ to be added to $\phi_s^{(i)0}$ along with $k^{(i)}\phi_s$, the portion of the bus flux that interacts with the i^{th} qubit, where $k^{(i)} = (L^{(i)}/L)$ with $L^{(i)}$ the inductance of the i^{th} coupling loop. For the case with no defects, we may write the Hamiltonian for the i^{th} perturbed qubit, with the definitions $c_{00} = \langle 0|\cos 2\psi|0\rangle$, $c_{11} = \langle 1|\cos 2\psi|1\rangle$, $s_{01} = \langle 0|\sin 2\psi|1\rangle$, $\varepsilon_j = \langle j|H_0|j\rangle/E_J$ as

$$\begin{aligned}
& \hat{1}^{bus} \otimes \hat{1}^{(i)} (H_0^{(i)} + H_1^{(i)} + H_{osc})/E_J \hat{1}^{(i)} \otimes \hat{1}^{bus} \\
& \cong \frac{1}{2}(\varepsilon_0 + \varepsilon_1)\hat{1}^{(i)} \otimes \hat{1}^{bus} + \frac{1}{2}(\varepsilon_0 - \varepsilon_1)\hat{\sigma}_z^{(i)} \otimes \hat{1}^{bus} + \hat{1}^{bus} \hbar\omega_{LC}/E_J (a_j^\dagger a_j + \frac{1}{2})\hat{1}^{bus} \otimes \hat{1}^{(i)} \\
& + \frac{1}{2}\rho M_\theta \dot{\phi}_a^{(i)2} \hat{1}^{(i)} \otimes \hat{1}^{bus} + \frac{1}{2}\rho M_\theta \dot{\phi}_s^{(i)2} \hat{1}^{bus} \otimes \hat{1}^{(i)} \\
& + \hat{1}^{bus} \{ \frac{1}{2}r(c_{00} + c_{11})[(J_0(\delta_a^{(i)}) - 1) + (J_0(\delta_s^{(i)}) - 1) - \tan\phi_s^0 J_0(\delta_a^{(i)})\sin\delta\phi_s^{(i)}] \} \hat{1}^{bus} \otimes \hat{1}^{(i)} \\
& + \hat{1}^{bus} \{ \frac{1}{2}r(c_{00} - c_{11})[(J_0(\delta_a^{(i)}) - 1) + (J_0(\delta_s^{(i)}) - 1) - \tan\phi_s^0 J_0(\delta_a^{(i)})\sin\delta\phi_s^{(i)}] \} \hat{1}^{bus} \otimes \hat{\sigma}_z^{(i)} \\
& + \{ \rho\dot{\phi}_a^{(i)}/(1+4\rho)2E_J \} \langle \Psi_0(\psi_i) | \partial/\partial\psi_i | \Psi_1(\psi_i) \rangle \hat{\sigma}_x^{(i)} \otimes \hat{1}^{bus} \\
& + \hat{1}^{bus} \{ r s_{01} (\cos\delta\phi_s^{(i)} \sin\delta\phi_a^{(i)} - \tan\phi_s^0 \sin\delta\phi_a^{(i)} \sin\delta\phi_s^{(i)}) \} \hat{1}^{bus} \otimes \hat{\sigma}_x^{(i)} \quad (3)
\end{aligned}$$

3.1 Logical Qubits for a Decoherence Free Subspace

The Rabi frequency $\Omega^{(i)}$ for coupling a bus excitation to the i^{th} qubit via the interaction term $\sin \delta\phi_a^{(i)} \sin \delta\phi_s^{(i)} \sigma_x^{(i)} \rightarrow \delta\phi_a^{(i)} \phi_s \sigma_x^{(i)}$ is given by $\Omega^{(i)} = [r \tan(\phi_s^0) \delta_a^{(i)} s_{10} \sqrt{\hbar \omega_{LC} L / 2} \mu(L^{(i)} / 2L)]$. Since $\Omega^{(i)} \propto 1/\sqrt{N}$, to increase $\Omega^{(i)}$ for a particular value of N it is necessary to increase either $\delta\phi_a^{(i)}$ or $L^{(i)}$ or both. Increasing $L^{(i)}$ (by forming multilevel spiral inductors) is only mildly effective due to the $(L^{(i)})^{\frac{1}{4}}$ dependence, while increasing the amplitude of $\delta\phi_a^{(i)}$, while effective has the drawback that the Bessel expansion term $r^{\frac{1}{2}}(\langle 0 | \cos 2\mu_i | 0 \rangle - \langle 1 | \cos 2\mu_i | 1 \rangle) ((J_0(\delta_a^{(i)}) - 1) \hat{\sigma}_z^{(i)} = \delta\Omega^{(i)} \hbar / E_J \hat{\sigma}_z^{(i)})$ is excited concomitantly, and will lead to phase errors when $\delta_a^{(i)}$ is not small.

This type of phase error (as well as any symmetric external flux fluctuations) can be nulled by using encoded logical product qubits with $\{|0_L\rangle = |01\rangle \equiv |0\rangle \otimes |1\rangle, |1_L\rangle = |10\rangle \equiv |1\rangle \otimes |0\rangle\}$ or by employing the two entangled Bell states $\{|\tilde{0}_L\rangle = (|01\rangle + |10\rangle)/\sqrt{2}, |\tilde{1}_L\rangle = (|01\rangle - |10\rangle)/\sqrt{2}\}$ as logical qubits. For either type, applying $\delta\phi_a^{(i)}$ and $\delta\phi_a^{(i+1)}$ to the first (i) and second ($i+1$) physical qubits of a logical qubit, will result in a positive phase shift in one physical qubit canceling a negative phase shift in the other if their two Rabi frequencies $\delta\Omega^{(i)}$ and $\delta\Omega^{(i+1)}$ are equal. It can be shown that this type of cancellation will occur during MS gates as well.

The Bell state qubits have the property that $t_r = \langle \tilde{0}_L | H^{(1)} + H^{(2)} | \tilde{1}_L \rangle = (\varepsilon_1 - \varepsilon_0)^{(1)} - (\varepsilon_1 - \varepsilon_0)^{(2)}$ and $\langle \tilde{0}_L | H^{(1)} + H^{(2)} | \tilde{0}_L \rangle = \langle \tilde{1}_L | H^{(1)} + H^{(2)} | \tilde{1}_L \rangle$, i.e. their eigen energies are exactly equal (if they are properly formed). However if the junction or flux properties of the two physical qubits differ, the transition matrix element t_r will be non zero and there will be tunneling between the two states. Transforming to a basis in which $t_r = 0$, yields the product states with zero tunneling but $\langle 0_L | H^{(1)} + H^{(2)} | 0_L \rangle - \langle 1_L | H^{(1)} + H^{(2)} | 1_L \rangle = (\varepsilon_1 - \varepsilon_0)^{(2)} - (\varepsilon_1 - \varepsilon_0)^{(1)}$ so there may be non zero time evolution.

3.2 Mølmer-Sørensen Gate

Sørensen and Mølmer have given a detailed description of a bichromatic excitation scheme that enables multiple qubit gate operations to be carried out for ion trap quantum computers^{8,9,10}. Their scheme is desirable since it allows for relatively rapid gates to be carried out via an oscillator bus, while returning the bus to its pre-gate initial configuration irrespective of the initial state of the bus. For the case of logical JJ prism qubits coupled by a resonant LC bus, the MS scheme is desirable since it allows logical qubit gates to be carried out without exciting figure 8 currents. As the gate operators for the ion-trap case have been set forth^{7,3} we display the needed gate operators for the slightly different case of the interaction Hamiltonian $\sin \delta\phi_a^{(i)} \sin \delta\phi_s^{(i)} \sigma_x^{(i)}$ while relaxing the condition that all qubit interactions have the same Rabi frequency. Expanding the $\sin \delta\phi_a^{(i)}$ and $\sin \delta\phi_s^{(i)}$ terms to lowest order in $\delta\phi_a^{(i)}$ and $\delta\phi_s^{(i)} = \frac{1}{2} \mu \phi_s (L^{(i)} / L)$ and making the rotating wave approximation leads to an interaction term $V(t) \cong -\sqrt{2} \Omega J_x(\vec{\phi}) [\varphi_s (\cos(\omega_{LC} - \delta)t + p_s (\sin(\omega_{LC} - \delta)t)] = J_x(\vec{\phi}) [f(t) \varphi_s + g(t) p_s]$

where $J_x(\vec{\phi}) = \frac{1}{2} \sum_i [e^{i\phi_i} \hat{\sigma}_+^i + e^{-i\phi_i} \hat{\sigma}_-^i] (\Omega_i / \Omega)$ with $\Omega_i = [r \tan(\phi_s^0) \delta_a^{(i)} s_{10} \sqrt{\hbar \omega_{LC} L / 2} \mu(L_{site} / 2L)]$ and Ω being the individual and average Rabi frequencies of the interacting qubits. For the MS bichromatic excitation, $\delta\phi_a^{(i)}$ is made up of signals from two microwave sources with source phases $\phi^{(i)}$ and frequencies $\omega_{\pm} = \omega_{10} \pm \delta$, where $\omega_{10} = (\varepsilon_1 - \varepsilon_0) / \hbar$ and $\delta \ll \omega_{LC} \pm 2\Omega$. In Ref. 10, the exact evolution operator for $V(t)$ is shown to be given exactly by

$$U(t) = \exp(-iA(t)J_x^2) \exp(-iF(t)J_x) \exp(-iG(t)J_x) \quad (4)$$

with $F(t) = \int_0^t f(\tau) d\tau = -\sqrt{2}\Omega \sin[(\omega_{LC} - \delta)t] / (\omega_{LC} - \delta)$, $G(t) = \int_0^t g(\tau) d\tau$ and $A(t) = -\int_0^t F(\tau)g(\tau) d\tau$. For a pulse length given by $(\omega_{LC} - \delta)t_K = 2\pi K$ where K is an integer, $F(t_K) = G(t_K) = 0$ and the bus can be returned to its initial vibrational state. Choosing values for K , δ , and Ω , yields $A(t_K) = -\Omega^2 2\pi K / (\omega_{LC} - \delta)^2$ and conversely $t_K = \sqrt{-A 2\pi K} / \Omega$. The single (logical) qubit gates can be composed as

$$\begin{aligned} \bar{X} &= 2J_x^2(\phi_{1,2} = 0) = \frac{1}{2}(\lambda_1^2 + \lambda_2^2)\hat{1} + \lambda_1\lambda_2\hat{\sigma}_x^{(1)}\hat{\sigma}_x^{(2)}, \\ \bar{Y} &= 2J_x^2(\phi_1 = 0, \phi_2 = \frac{1}{2}\pi) = \frac{1}{2}(\lambda_1^2 + \lambda_2^2)\hat{1} - \lambda_1\lambda_2\hat{\sigma}_x^{(1)}\hat{\sigma}_y^{(2)} \end{aligned} \quad (5)$$

where $\lambda_i = \Omega_i / \Omega$. Operators for product and Bell logical qubits are given respectively by $\{\sigma_{Lx} = \sigma_x^{(1)}\sigma_x^{(2)}, \sigma_{Ly} = \sigma_y^{(1)}\sigma_x^{(2)}, \sigma_{Lz} = -i\sigma_{Lx}\sigma_{Ly}\}$ and $\{\tilde{\sigma}_{Lx} = -i\tilde{\sigma}_{Lx}\tilde{\sigma}_{Ly}, \tilde{\sigma}_{Ly} = -\sigma_y^{(1)}\sigma_x^{(2)}, \tilde{\sigma}_{Lz} = \sigma_x^{(1)}\sigma_x^{(2)}\}$. For the product logical qubits, the CZ gate may be written as $U_{CZ}^{(I,II)} = \sqrt{i} \exp(i\sigma_{Lz}^{(I)}\sigma_{Lz}^{(II)}\pi/4) \exp(-i\sigma_{Lz}^{(I)}\pi/4) \exp(-i\sigma_{Lz}^{(II)}\pi/4)$ where the term $\exp(i\sigma_{Lz}^{(I)}\sigma_{Lz}^{(II)}\pi/4)$ can be expressed in terms of a four (physical) qubit Mølmer-Sørensen gate $\overline{XX} = 2J_x^2(\phi_{1,2,3,4} = 0)$

$$U_{CZ}^{(I,II)} = \exp(i\pi/4) \exp(i\overline{XX}\pi/4) \exp(i\sigma_{Lz}^{(I)}\pi/4) \exp(i\sigma_{Lz}^{(II)}\pi/4) \quad (6)$$

When the Rabi frequencies for the four physical qubits are not identical, mixed terms like $\sigma_x^1\sigma_x^4$ will arise with non zero coefficients proportional to $\gamma_i = \lambda_i - 1$. If the Rabi frequencies for each physical qubit of a logical qubit pair can be made equal, then Ω can be defined as the average Rabi frequency with $\gamma = \gamma_1 = \gamma_2 = -\gamma_3 = -\gamma_4$. Terms that are proportional to $\gamma_1 + \gamma_2 + \gamma_3 + \gamma_4$ will be nulled, and the remaining terms will be proportional to either $\sigma_x^{(1)}\sigma_x^{(2)}$, $\sigma_x^{(3)}\sigma_x^{(4)}$, or $\sigma_x^{(1)}\sigma_x^{(2)}\sigma_x^{(3)}\sigma_x^{(4)}$ that can be accommodated by small changes in pulse lengths. If the two Rabi frequencies $\delta\Omega^{(i)}$ and $\delta\Omega^{(i+1)}$ for each logical qubit pair are equal, as is required to cancel out $\delta\Omega^{(i)}\hat{\sigma}_z^{(i)}$ and $\delta\Omega^{(i+1)}\hat{\sigma}_z^{(i+1)}$ phase errors generated during a gate, then $j_c^{(1)} \cos(\phi_{s0}^{(1)}) (c_{00}^{(1)} - c_{11}^{(1)}) [\delta_a^{(1)}]^2 = j_c^{(2)} \cos(\phi_{s0}^{(2)}) (c_{00}^{(2)} - c_{11}^{(2)}) [\delta_a^{(2)}]^2$ is satisfied. If

$j_c^{(1)} \sin(\phi_{s_0}^{(1)}) s_{01}^{(1)} [\delta_a^{(1)}] = j_c^{(2)} \sin(\phi_{s_0}^{(2)}) s_{01}^{(2)} [\delta_a^{(2)}]$ is satisfied, then the Rabi frequencies for qubits 1 and 2 will be equal. For both constraints to hold concurrently, the equality of Eq. (7) must be satisfied, which is possible to achieve by varying $\delta_a^{(1)}$ (or $\delta_a^{(2)}$) if $\phi_{s_0}^{(1)}$ and

$$(\delta_a^{(2)} / \delta_a^{(1)}) = \tan(\phi_{s_0}^{(2)}) s_{01}^{(2)} (c_{00}^{(1)} - c_{11}^{(1)}) / \tan(\phi_{s_0}^{(1)}) s_{01}^{(1)} (c_{00}^{(2)} - c_{11}^{(2)}) = f(r^{(1)}, r^{(2)}) \quad (7)$$

$\phi_{s_0}^{(2)}$ are fixed, as shown in Fig. (3).

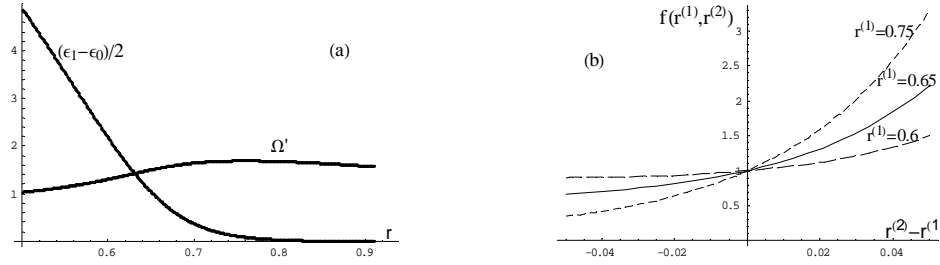


Figure 3. a) $\frac{1}{2}$ Transition frequency (for $E_J / \hbar = 200GHz$) and const. \times Rabi frequency Ω vs. r .
b) $f(r^{(1)}, r^{(2)})$ as a function of $r^{(2)} - r^{(1)}$ for $r^{(1)} = 0.60, 0.65,$ and 0.75 .

4. CIRCULATING CURRENT PATTERNS FOR THE QUBIT STATES

The circulating current patterns associated with the $|0\rangle$ and $|1\rangle$ states can be derived by using $\zeta_{3,4} = 2\psi - \phi_a \mp \phi_s$ and by assuming ϕ_a to be a small perturbation, which then yields

$$\begin{aligned} J_{3,4}^{|0\rangle} &= \langle 0 | J_{C3,4} \sin \zeta_{3,4} | 0 \rangle = \mp j \kappa_0 (1 \pm \cos \phi_s^0 \sin \phi_a / \sin \phi_s^0 \cos \phi_a) \\ J_{3,4}^{|1\rangle} &= \langle 1 | J_{C3,4} \sin \zeta_{3,4} | 1 \rangle = \mp j \kappa_1 (1 \pm \cos \phi_s^0 \sin \phi_a / \sin \phi_s^0 \cos \phi_a) \end{aligned} \quad (8)$$

with $\kappa_0 = \sin \phi_s^0 \cos \phi_a^0 \langle 0 | \cos 2\psi | 0 \rangle$ and $\kappa_1 = \sin \phi_s^0 \cos \phi_a^0 \langle 1 | \cos 2\psi | 1 \rangle$. In the Hartree approximation if $\Delta J = \Delta j = 0$ the expectation value of $J_1 = J_{C1} \sin \zeta_1$ in the $|1\rangle$ or $|0\rangle$ state of ψ is equal to zero. The circulating current patterns associated with the unperturbed $|0\rangle$ and $|1\rangle$ states are thus clockwise currents of magnitude $J_3^{|0\rangle} = -J_4^{|0\rangle} = -j \kappa_0$ and $J_3^{|1\rangle} = -J_4^{|1\rangle} = -j \kappa_1$ around the perimeter of the qubit, and are plotted vs. r in Fig. 7b.

Since the probability density for the two superposition states $|\pm\rangle = \frac{1}{\sqrt{2}}(|0\rangle \pm |1\rangle)$ is centered around the potential well minima at $\psi = \mp \psi^*$, circulating currents for these states are close to the classical equilibrium currents. Writing $\kappa_{01} = \langle 0 | \sin 2\psi | 1 \rangle \cos(\phi_s^0 - \phi_a^0)$, circulating currents for the $|\pm\rangle$ states may be reexpressed as

$$\begin{aligned}
J_3^{|\pm\rangle} &= \langle \pm | J_{C3} \sin \zeta_3 | \pm \rangle = -\frac{1}{2} j(\kappa_0 + \kappa_1) + j\kappa_{01}, & J_3^{|\mp\rangle} &= \langle \mp | J_{C3} \sin \zeta_3 | \mp \rangle = -\frac{1}{2} j(\kappa_0 + \kappa_1) - j\kappa_{01} \\
J_4^{|\pm\rangle} &= \langle \pm | J_{C4} \sin \zeta_4 | \pm \rangle = +\frac{1}{2} j(\kappa_0 + \kappa_1) + j\kappa_{01}, & J_4^{|\mp\rangle} &= \langle \mp | J_{C4} \sin \zeta_4 | \mp \rangle = +\frac{1}{2} j(\kappa_0 + \kappa_1) - j\kappa_{01}.
\end{aligned} \tag{9}$$

The circulating current is thus comprised of a perimeter current $\frac{1}{2}j(\kappa_0 + \kappa_1)$, which has the same sign for the $|\pm\rangle$ states, and a figure eight current $j\kappa_{01}$ that changes sign for $|\pm\rangle$ states.

4.1 Initializing the Qubits and the Effect of Critical Current and Geometric Defects

All of the qubits are initially allowed to relax to their respective ground states. For a system in which all of the cell and junction parameters are identical, every even numbered qubit is given an x rotation of 180° . In order to avoid phase errors during these initializing single qubit gates, the gates should be carried out with long, small amplitude microwave pulses. Each $\{i_{\text{odd}}, i_{\text{odd}+1}\}$ pair of qubits is then designated as a product logical qubit {I,II,III..}. To initialize the Bell state logical qubits a further logical (MS) Hadamard gate is needed for each logical qubit. A test measurement should show that there is no antisymmetric flux coupled to the SQUID gradiometer detectors

For a qubit in which there is some combination of junction critical current defects and cell geometry defects, a term in the Hamiltonian will be generated that is antisymmetric in ψ and θ

$$\begin{aligned}
\Delta V &= -\{2j \sin \phi_{a,geom} \cos \phi_s^0 + 2\Delta j \cos \phi_{a,geom} \sin \phi_s^0\} \sin 2\psi - 2\Delta J \sin \theta \sin \psi \\
&= -\kappa_{defect} \sin 2\psi - 2\Delta J \sin \theta \sin \psi = \Delta V^a + \Delta V^b
\end{aligned} \tag{10}$$

The effect of ΔV^a on the potential is to tilt it in the ψ direction as shown in Fig. 4b, while the effect of ΔV^b is to skew the potential as shown in Fig. 4c. For ΔV^b an accurate numerical solution for the 2D potential has been undertaken but not yet completed, we will thus approximate the perturbed wavefunctions using first order perturbation theory.

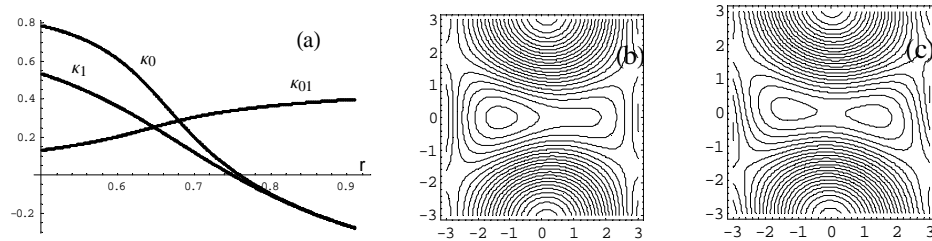


Figure 4a. a) Symmetric $\{\kappa_0, \kappa_1\}$ and antisymmetric $\{\kappa_{01}\}$ current amplitudes vs. r .

b) Contour plot of $V(\theta, \psi)$ for $\Delta V_a \neq 0$. c) Contour plot of $V(\theta, \psi)$ for $\Delta V_b \neq 0$.

In a Hartree approximation there are four types of states when labeled by parity with respect to θ and ψ ; $|m, n\rangle = \{|even, even\rangle, |even, odd\rangle, |odd, even\rangle, \text{ and } |odd, odd\rangle\}$ where m and n are the number of nodes in θ and ψ . The only type of (separable) states contributing to the summation that will survive in a first order perturbation

expansion $|\mathbf{n}\rangle = |\mathbf{n}^0\rangle + \sum_{k \neq n} \langle \mathbf{k}^0 | \Delta V^b | \mathbf{n}^0 \rangle / (E_n^0 - E_k^0)$ for $|0\rangle$ and $|1\rangle$, are $|odd, odd\rangle$ and $|odd, even\rangle$ type states respectively, where $|\mathbf{n}^0\rangle$ are unperturbed states. Keeping only the lowest energy terms $|2^0\rangle = |1, 1\rangle$ and $|3^0\rangle = |1, 0\rangle$, an approximate solution may be written as $|0\rangle = |0^0\rangle + \alpha |2^0\rangle$ and $|1\rangle = |1^0\rangle + \beta |3^0\rangle$ where $\alpha = 2\Delta J \langle 2^0 | \sin\theta \sin\psi | 0^0 \rangle / (E_2^{(0)} - E_0^{(0)})$ and $\beta = 2\Delta J \langle 3^0 | \sin\theta \sin\psi | 1^0 \rangle / (E_3^{(0)} - E_0^{(0)})$. The matrix elements of ΔV^b are then given by $\langle 0 | \Delta V^b | 0 \rangle = 2\alpha \langle 0^0 | \Delta V^b | 2^0 \rangle$, $\langle 1 | \Delta V^b | 1 \rangle = 2\beta \langle 1^0 | \Delta V^b | 3^0 \rangle$, and $\langle 0 | \Delta V^b | 1 \rangle = 0$. Critical current defects in junctions 1 and 2 will thus lead to a second order (in $\Delta J / J$) correction in the energies of the two qubit states, but it will not lead to transitions between them.

The most direct way of nulling the ΔV^a term is to add a small external antisymmetric ‘trim’ flux to the existing flux so that the resultant antisymmetric flux $\phi_a^0 = \phi_{a,geom} + \phi_{a,trim}$ will satisfy $\tan\phi_a^0 = -(\Delta j / j) \tan\phi_s^0$. The net result of having $\phi_a^{(0)}$ determined by this equation, is that small figure eight currents that were present initially in the $|0\rangle$ and $|1\rangle$ states and could interact with the SQUID detector are now nulled, while perimeter currents in the $|0\rangle$ and $|1\rangle$ states will be slightly decreased by the last factor in Eq. (8) which simplifies to $(1 \pm \Delta j / j)(1 \mp \cos\phi_s^0 \sin\phi_a / \sin\phi_s^0 \cos\phi_a) = [1 - (\Delta j / j)^2]$. If $\Delta J / J$ is not zero, then there will be a multiplicative factor of $(1 + \alpha^2 c_{00} / c_{00})$ for the $|0\rangle$ state and $(1 + \beta^2 c_{00} / c_{11})$ for the $|1\rangle$ state.

If the trim current is not applied, then there will be a non zero figure eight current of magnitude $\kappa_0(\Delta j + j \tan\phi_{a,geom} / \tan\phi_s^0)$ for the $|0\rangle$ state and $\kappa_1(\Delta j + j \tan\phi_{a,geom} / \tan\phi_s^0)$ for the $|1\rangle$ state. From Fig. 4a it can be seen that if the qubit is operated around r^* , then κ_0 and κ_1 are small (\sim equal and opposite) and Ω_{Rabi} is near its maximum at $r \approx 0.75$.

The Hamiltonian $H_0 + \Delta V$ can be diagonalized by a unitary rotation to a new basis. Since the unperturbed wave functions for the two basic states $\Psi_0(\theta, \psi) = \langle \theta, \psi | 0 \rangle$ and $\Psi_1(\theta, \psi) = \langle \theta, \psi | 1 \rangle$ are both symmetric in θ , the matrix element of the last term in ΔV will be zero. Only junction defects Δj , associated with outer junctions 3 and 4, and a small antisymmetric flux ϕ_a due to different cell sizes, will then affect the operation of the qubit.

4.2 Connecting Buses into a Network

It is possible to couple groups of buses in an open branching network using transfer qubits as first described in Ref. (4). A diagram of one possible coupling scheme is shown in Fig. 1c where bus 1 is coupled symmetrically to the transfer qubit and bus 2 is coupled antisymmetrically in order to prevent direct mutual inductance coupling from bus 1 to bus 2. Using $\tilde{U}_{CN}^{(I,II)}$ from Eq. (6), an expression for $\tilde{U}_{CN}^{(j,k)}$ may be written using the Hadamard operator \tilde{H}_k as $\tilde{U}_{CN}^{(j,k)} = \tilde{H}_k \tilde{U}_{CN}^{(j,k)} \tilde{H}_k$. Writing $\tilde{H}_k = -ie^{-i(\pi/4)\tilde{\sigma}_{L_y}^{(k)}} e^{i(\pi/2)\tilde{\sigma}_{L_z}^{(k)}}$, the $\tilde{C}\tilde{N}$ operator may be expressed as $\tilde{U}_{CN}^{(j,k)} = e^{-i(\pi/4)\tilde{\sigma}_{L_y}^{(k)}} \tilde{U}_{CN}^{(j,k)} e^{i(\pi/4)\tilde{\sigma}_{L_y}^{(k)}}$ which requires 4 (bichromatic) microwave pulses. Since $\{x_{(1)}, p_{(1)}\}$ commute with $\{x_{(2)}, p_{(2)}\}$, the

expression for $A(t)$ in Eq. 4. is replaced by $A(t) \rightarrow A_{(1)}(t) + A_{(2)}(t)$. For both bus oscillators to return to their pre gate values both of the constraints $(\omega_{(1)LC} - \delta)t_K = K_{(1)}2\pi$ and $(\omega_{(2)LC} - \delta)t_K = K_{(2)}2\pi$ with integer $K_{(i)}$ must be satisfied simultaneously. For $K_{(2)} = -K_{(1)}$ a solution is $\delta = (\omega_{(1)LC} + \omega_{(2)LC})/2$, $t_K = 4\pi K_{(1)} / (\omega_{(1)LC} - \omega_{(2)LC})$, which yields $A_{(2)}(t) = -A_{(1)}(t)(-1)^P$ where P is the parity of the bus 1-bus2 coupling. Thus $U(t_K) = \exp(-2iA_{(1)}(t_K)\sigma_x^{(1)}\sigma_x^{(2)})$.

For the 2 logical qubit CZ gate, if one of the logical qubits is a transfer qubit, its coupling to a second bus will engender a single logical qubit rotation that is in the proper direction for the CZ gate. Thus if logical qubit 3-4 is a transfer qubit connected to a second bus, the expression $\exp(i\pi\overline{XX}/4) = \exp(-i\pi/4)\exp(-i\pi\hat{\sigma}_x^{(1)}\hat{\sigma}_x^{(2)}\hat{\sigma}_x^{(3)}\hat{\sigma}_x^{(4)}/4)$ picks up a factor $\exp[i\pi\hat{\sigma}_x^{(3)}\hat{\sigma}_x^{(4)}/4]$ obviating the necessity a separate gate. If there are two transfer qubits involved, no single logical qubit gates are needed at the transfer qubit sites. This reduces the number of separate microwave pulses for a CN gate with one bus transfer from 5 to 3 and also reduces the time needed to carry out the gate by $2t_K$.

To carry out a CN gate over a number of buses, it is necessary to first carry out a sequence of $\tilde{U}_{CN}^{(j,i)}$'s starting from the control qubit, through all of the intervening transfer qubits to the target qubit, followed by a final sequence of $\tilde{U}_{CN}^{(i,i')}$ from the original qubit to the last transfer qubit in order to reset the transfer qubits to their original ground states. The sequence involving 2 transfer qubits would thus be $\tilde{U}_{CN}^{(i,i')}$ between $(j,t_1), (t_1,t_2), (t_2,k)$ followed by resetting transfer qubits with $\tilde{U}_{CN}^{(i,i')}$ applied to (j,t_1) and (t_1, t_2) . These maneuvers may be chained across as many coupled buses as required. The wave equation for the entire system may be written as $|\Psi\rangle = \sum_n c_n |\Psi_n^n\rangle$ with $|\Psi_n^n\rangle = \prod_{i=1}^N |\tilde{\chi}_{\alpha_i}^{(i)}\rangle \otimes \prod_{j=1}^{N_r} |\tilde{\chi}_{\beta_j}^{(j)}\rangle \otimes \prod_{k=1}^{N_{bus}} |\chi_{(k),\gamma_k}\rangle$, where the qubits and bus are restricted to the two lowest energy states $\alpha_i = \{0,1\}$, $\beta_j = \{0,1\}$, $\gamma_k = \{0,1\}$ and where $\mathbf{n} = \{\alpha_1, \alpha_2, \dots, \alpha_N, \beta_1, \beta_2, \dots, \beta_{N_r}, \gamma_1, \gamma_2, \dots, \gamma_{N_{bus}}\}$ with $|\tilde{\chi}_0\rangle = |\tilde{0}_L\rangle$, $|\tilde{\chi}_1\rangle = |\tilde{1}_L\rangle$, $|\chi_0\rangle = |0_{Bus}\rangle$, and $|\chi_1\rangle = |1_{Bus}\rangle$. Because the MS gates return the buses and (along with resetting) the transfer qubits to the initial state they were in before the $\tilde{U}_{CN}^{(j,k)}$ gate, and the logical qubits do not evolve in time, it should be possible to maintain quantum coherence across the set of coupled buses. This allows open branching networks of coupled buses to be formed, enlarging the possible number of interacting qubits in a single quantum computer.

CONCLUSIONS:

We have shown that it is possible to design a quantum computer comprised of Josephson junction prism qubits that are coupled via the flux of a resonant LC bus. that is capable of carrying out quantum computations in a decoherence free subspace. The effective Hamiltonian is zero between gates, so there is no dynamical evolution of the system. The $|0\rangle$ and $|1\rangle$ physical qubit states are characterized by circulating currents that follow the perimeter of a two cell qubit, and are thus symmetric with respect to the flux threading the cells of the qubit. The logical qubit states are made up of linear

combinations of $|01\rangle \equiv |0\rangle \otimes |1\rangle$ and $|10\rangle \equiv |1\rangle \otimes |0\rangle$, with the result that no antisymmetric currents or fluxes are generated by the qubits when Mølmer-Sørensen gates are employed. A coupled SQUID gradiometer that is antisymmetric with respect to the flux threading the two cells of a qubit will not register any coupled flux until a Hadamard transform is carried out on the physical qubits, immediately prior to a measurement. The two basic states are then transformed into \pm combination states that have antisymmetric ‘figure 8’ circulating currents whose flux is then measurable by the SQUID gradiometer. The coupling of each qubit to an LC resonant bus is made by means of a loop that encircles both cells of the qubit symmetrically. This prevents the direct mutual inductance coupling of the bus to both antisymmetric microwave gate pulses and the measuring SQUID gradiometer.

Pairing the qubits into logical qubits also enables Mølmer-Sørensen gates to be used, since the phase errors that would ensue if QC were based on physical qubits are cancelled out in each pair of qubits. The requirement that the LC resonant loop be smaller in extent than one tenth of a substrate wavelength to remain within the quasistatic limit, constrains the number of qubits that can interact on a single LC resonant bus to around $N = \sim 50 - 100$. To enlarge the system, two resonant loop buses are coupled by means of a ‘transfer’ logical qubit that couples concurrently to both buses. Direct interaction of the loops is prevented by coupling them antisymmetrically. With more than one transfer qubit per bus, the buses may be coupled into a scalable open network. The use of Mølmer-Sørensen gates insures that the quantum states of the buses and transfer qubits will be returned to their pre-gate status. Since the logical qubits do not evolve in time, it should be possible for the system of coupled buses and qubits to maintain quantum coherence.

ACKNOWLEDGEMENTS:

The author appreciates helpful conversations with Alexey Ustinov, Farrukh Abdumalikov, Will Oliver, Al Drehman, and Jianke Yang. This work was carried out with support from Air Force Office of Scientific Research AFOSR.

REFERENCES :

1. J. I. Cirac and P. Zoller Phys. Rev. Lett. **74**, 4091, (1995).
2. Y. Makhlin, G. Schön, and A. Shnirman, Rev. Mod. Phys. **73**, 357, (2001)
3. O. Buisson and F. W. Hekking, in *Macroscopic Quantum Coherence and Quantum Computing* (Kluwer Academic, Dordrecht), p137, (2001).
4. S. Yukon, Physica C **368**, 320 (2002).
5. M. J. Feldman and X. Zhou, in *Quantum Computing and Quantum Bits in Macroscopic Systems* (Kluwer Academic, Dordrecht), p219, (2004).
6. D. Bacon, J. Kempe, D. A. Lidar, and K. B. Whaley, Phys. Rev. Lett. **85**, 1758 (2000)
7. D. Bacon, Decoherence, Control and Symmetry in Quantum Computers, Phd. Thesis, Cal. Inst. Tech. 1997.
8. A. Sørensen and K. Mølmer, Phys Rev. Lett. **82**, 1971 (1999).
9. K. Mølmer and A. Sørensen, Phys Rev. Lett. **82**, 1835 (1999).
10. A. Sørensen and K. Mølmer, Phys A **62**, 1022311 (2000).
11. Mooij, J.E., T.P. Orlando, L. Levitov, L. Tian, C. H. van der Wal, and S. Lloyd, Science, **285**, 1036 (1999), , Science **290**, 773, (2000).
13. D. S. Crankshaw and T. P. Orlando, IEEE Trans. on Appl. Sup. **11**, 1006, (2001).
14. K. M. Unwin, F. M. Arscott, Proc. Roy Soc. Edinb. **71**, 28, (1971).

Stanford P. Yukon
Air Force Research Laboratory/SNHE
Electromagnetics Technology Division
80 Scott Road
Hanscom AFB, MA. 01731 U.S.A.

Email: yukon@hanscom.af.mil
Tel: 781-377-2968
Fax: 781-235-2717